0.1 Nuclear Structure in a nutshell

The low–energy properties of quantal, many–body, Fermi systems displaying sizable values of zero–point–motion (kinetic energy) of localization compared to the strength of the NN–interaction and quantified by a quantality parameter $Q \gtrsim 0.15$, are determined by the laws which control independent particle motion close to the Fermi energy ϵ_F (on–the–energy shell), and by the correlations operating among them.

First of all, the Pauli principle, implying orbitals solidly anchored to the singl–particle mean field, as testified by the Hartree–Fock ground state $|HF\rangle = \Pi_i a_i^\dagger|0\rangle$, describing a step function separation in the probability of occupied ($\epsilon_i \leq \epsilon_F$) and empty ($\epsilon_k \geq \epsilon_F$) states (box 1).

Pairing acting on fermions moving in time reversal states lying close to ϵ_F alters this picture in a conspicuous way. In particular, in the case of $S = 0$ configurations, in which case the radial component of the pair wavefunction does not display nodes. Within an energy range of the pair correlation energy $E_{corr}(\approx 2\Delta$ within BCS) centered around $\epsilon_F(E_{corr}/\epsilon_F \ll 1)$ the system is now made out of pairs of fermions which flicker in and out of the correlated ($L = 0, S = 0$) configuration (Cooper pairs, box 2). For temperatures (intrinsic excitation energies) or stress regimes (magnetic field in metals, Coriolis force in nuclei, etc.) smaller than $\approx E_{corr}/2$ (critical value), Cooper pairs respect Bose–Einstein statistics, the single–particle orbits on which they are correlated become dynamically detached from the mean field, leading to a bosonic condensate and, at the same time, reducing in a conspicuous way the inertia of the system (e.g. the moment of inertia $\mathcal{I}$ of quadrupole rotational bands is much smaller than the rigid moment of inertia ($\mathcal{I} \approx \mathcal{I}/3$) expected from independent particle motion). Cooper pairs exist also in situation in which the environmental condition are above critical, e.g. in metals at room temperature or nuclei at high values of the angular momentum, although they break as soon as they are generates (pairing vibrations). While these pair addition and substraction fluctuations have little effect on condensed systems, they play an important role in mesoscopic systems, in particular in nuclei (box 3).

Within the rfamework of the above picture, one can introduce at profit a collective coordinate α_0 (order parameter) which measures the number of Cooper pairs participating in the pairing condensate, and define a wavefunction for each pair $\left(U_\nu + V_\nu a_\nu^\dagger a_{\bar{\nu}}^\dagger\right)|0\rangle$ (independent pair motion, BCS approximation), adjusting the occupation parameters V_ν and U_ν (probability amplitudes that the two–fold (Kramer's–)degenerate pair state $(\nu, \bar{\nu})$ is either occupied or empty), so as to minimize the energy of the system under the condition that the average number of nucleons is equal to N_0 (Coriolis force felt, in the inrinsic system, by the pairs, equal to $-\lambda N_0$). Thus, $|BCS\rangle = \Pi_{\nu>0}\left(U_\nu + V_\nu a_\nu^\dagger a_{\bar{\nu}}^\dagger\right)|0\rangle$ provides a valid description of the paired mean field ground state, and of the associated order parameter $\alpha_0 = \langle BCS|P^\dagger|BCS\rangle$, $P^\dagger = \sum_{\nu>0} a_\nu^\dagger a_{\bar{\nu}}^\dagger$ being the pair creation operator (box 2).

It is then natural to posit that two–nucleon transfer reactions are specific to probe pairing correlations in many–body fermionic systems. Examples are provided by the Josephson effect in e.g. metallic superconductors, and (t, p) and (p, t) reactions in atomic nuclei.

Because away from the Fermi energy pair independent motion becomes independent particle motion, in particular in the nuclear case $|BCS\rangle \to |\text{Nilsson}\rangle$, one–particle transfer reactions like e.g. (d, p) and (p, d) can be used together with (t, p) and (p, t) processes as a valid tool to cross check pair correlation predictions. In particular, to shed light on the origin of pairing in nuclei: in a nutshell, the relative importance of the bare NN–interaction and the induced pairing interaction (box 4).

While the calculation of two–nucleon transfer spectroscopic amplitudes and differential cross sections are, a priori, more involved to be worked out than those associated with one–nucleon transfer reactions, the former are, as a rule, more intrinsically accurate than the later ones. This is because in the first case, the actual value of the variety of quantities reflect coherence, and thus the averaging over many contributions $\sqrt{j + 1/2}\, U_\nu V_\nu$ thus the averaging which, in spite of the fact that each of them may be somewhat inaccurate, they overall sum leads to $\alpha_0(d\sigma(2\text{n–transfer})/d\Omega \sim |\alpha_0|^2)$. On the other hand, $(d\sigma(1\text{n–transfer})/d\Omega \sim |U_\nu|^4$ or $\sim |V_\nu|^2$ thus depending on the accuracy with which one is able to calculate the occupancy of a pure configuration (box 4).

The above parlance is reflected in the calculation of the elements resulting from the encounter of structure and reaction, namely one– and two–nucleon modified transfer formfactors. While it is usually considered that these quantities carry all the structure information associated with the calculation of the corresponding cross sections, a consistent NFT calculation of structure and reaction will posit that equally much is contained in the distorted waves describing the relative motion of the colliding systems. This is because the optical potential $(U + iW)$ which determines these scattering waves, emerges from the same modified formfactors, eventually including also inelastic processes. In other words, setting detectors in e.g. a definite two–particle transfer channel like $A + t \to B(= A + 2) + p$, one needs to know what the single–particle states and collective modes of the systems $F(= A + 1)$ and A and B are respectively, as well as their interweaving leading to dressed particle states (quasiparticles; fermions) are renormalized normal modes of excitation (bosons) are. But these are essentially all the elements needed to calculate the processes leading to the depopulation of the flux of the incoming channel ($A + t$ in the case under discussion). In particular, and assuming to work with spherical nuclei, so as to avoid strong inelastic processes, one–particle transfer is, as a rule (in particular Q–value closed channels) the main depopulation process, in keeping with the long range tail of the associated formfactor as compared to that of other processes.

In keeping with this fact, and because U and W are connected by the Kramers–Krönig generalized dispersion relation (fluctuation dissipation theorem), it is possible to calculate the nuclear dielectric function (optical potential) needed to describe the $A + a \to B + p$ process in question.

Concerning the modified formfactor associated with this process, we shall see in the next Chapter that it can be written as

$$U^{J_iJ_f}_{LSJ}(R) = \sum_{\substack{n_1l_1j_1\\ n_2l_2j_2}} B(n_1l_1j_1, n_2l_2j_2; JJ_iJ_f)$$
$$\langle SLJ|j_1j_2J\rangle\langle no, NL, L|n_1l_1, n_2l_2; L\rangle$$
$$\Omega_n R_{NL}(R)$$

where the overlaps

$$B(n_1l_1j_1, n_2l_2j_2; JJ_iJ_f)$$
$$=\langle\Psi^{J_f}(\xi_{A+2})|\left[\phi^J(n_1l_1j_1, n_2l_2j_2), \Psi^{J_i}(\xi_A)\right]^{J_f}\rangle$$

and

$$\Omega_n = \langle\phi_{nlm_l}(\mathbf{r})|\phi_{000}(\mathbf{r})\rangle$$

encodes for the physics of particle–particle (but also, to a large extent, particle–hole) correlations in nuclei, $\langle SLT|j_1j_2J\rangle$ and $\langle no, NL, L|n_1l_1, n_2l_2; L\rangle$ being $LS - jj$ and Moshinsky transformation brackets, keeping track of symmetry and number of degrees conservation. In fact, the two–nucleon spectroscopic amplitude (B–coefficient) and the overlap Ω_n reflect the parentage in which the nucleus B can be written in terms of the system A and a Cooper pair,

$$\Psi_{exit} = \Psi^{J_f}_{M_f}(\xi_{A+2})\chi^{S_f}_{M_{sf}}(\sigma_p),$$

where

$$\Psi^{J_f}_{M_f}(\xi_{A+2}) = \sum_{\substack{n_1l_1j_1\\ n_2l_2j_2\\ J,J'_i}} B(n_1l_1j_1, n_2l_2j_2; JJ_iJ_f)$$
$$= \left[\phi^J(n_1l_1j_1, n_2l_2j_2)\Psi^{J'_i}(\xi_A)\right]^{J_f}_{M_f}$$

and

$$\Psi_{entrance} = \Psi^{J_i}_{M_i}(\xi_A)\phi_t(\mathbf{r}_{n1}, \mathbf{r}_{n2}, r_p; \sigma_{n1}, \sigma_{n2}, \sigma_p)$$

with

$$\phi_t = \left[\chi^S(\sigma_{n1}, \sigma_{n2})\chi^{S'f}(\sigma_p)\right]^{S_i}_{M_si}\phi^{L=0}_t\Big(\sum_{i>j}|\mathbf{r}_i - \mathbf{r}_j|\Big)$$

Assuming for simplicity a symmetric di–neutron radial wavefunction of the triton, i.e. neglecting the d–component of the corresponding wavefunction, for the relative and center of mass wavefunctions $P_{nlm}(\mathbf{r})$ and $\Phi_{N\Lambda M}(R)$ ($n = l = m = 0, N = \Lambda = M = 0$), leads to Ω_n, a quantity that reflects both the non–orthogonality existing between the di–neutron wavefunctions in the final nucleus (Cooper pair) and in the triton. Another way to say the same thing is that dineutron correlations in these two systems are different, a fact which underscores the limitations of the light ion reactions to probe specifically pairing correlations in nuclei.

One can then conclude that, provided one makes use of a (sensible) complete single–particle basis (eventually including also the continuum), one can capture through $U^{J_iJ_f}_{LSJ}(R)$ most of the coherence of Cooper pair transfer, in keeping with ht fact that major aspects of the associated di–neutron non–locality are taken care of by the n–summation weighted by the non–orthogonal overlaps Ω_n. This is in keeping with the fact that, making use of a more refined triton wavefunction than employed above, the $n-p$ (deuteron–like) correlations of this particle can be described with reasonable accuracy and thus the emergence of successive transfer. On the other hand, being the deuteron a bound system, this effective treatment of the associated resonances is not particular economic. Furthermore, zero–range approximation ($V(\rho)\phi_{000}(\rho) = D_0\delta(\vec{\rho})$) blocks such a possibility.

Nonetheless, the fact that one can still work out a detailed and consistent picture of two–nucleon transfer reactions in nuclei in terms of absolute cross sections with the help of a single parameter ($D_0^2 \approx (31.6 \pm 9.3)10^4\text{MeV}^2\text{fm}^2$) testifies to the fact that the above picture of Cooper pair transfer is a powerful picture, as it contains a large fraction of the physics which is at the basis of Cooper pair transfer in nuclei (Broglia et al. (1973); Ch. 2). This is the reason why,treating explicitly the intermediate deuteron channel in terms of successive transfer, correcting both this and the simultaneous transfer channel for non–orthogonality contributions, makes the above picture the quantitative probe of Cooper pair correlations in nuclei (Potel et al. (2013); Ch. 4 and 5), as testified by Fig. **??** and Table **??**. Within this context, we provide below two examples of B–coefficients. One for the case in which A and $B(=A+2)$ are members of a pairing rotational ...

$$B(nlj,nlj;000) = \langle BCS(N+2)|[a^\dagger_{nlj}a^\dagger_{nlj}]^0_0|BCS(N)\rangle = \sqrt{j+1/2}\,U_{nlj}(N)V_{nlj}(N+2)$$

and

$$\begin{aligned} B(nlj,nlj;000) =& \langle N_0+2(gs)|[a^\dagger_{nlj}a^\dagger_{nlj}]^0_0|N_0(gs)\rangle \\ =& \begin{cases} \sqrt{j+1/2}X_a(n_kl_kj_k) & (\epsilon_{j_k} > \epsilon_F) \\ \sqrt{j+1/2}Y_a(n_il_ij_i) & (\epsilon_{j_k} \leq \epsilon_F) \end{cases} \end{aligned}$$

For actual numerical values see box 3 and Tables

$\boxed{\text{Quantality parameter}}$ ratio of quantal kinetic energy of localization and potential energy; $\boxed{\text{box 1}}$ App. 2.A

$$Q = \frac{\hbar^2}{M_n a^2}\frac{1}{|v_0|}; \quad M_n = 0.939\ \text{GeV}/c^2 \ \text{(neutron mass)}$$

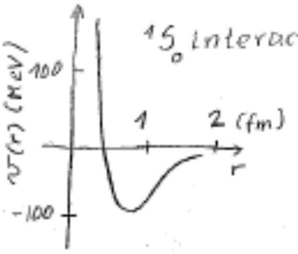

$a \approx 1$ fm (range)

$v_0 \approx -100$ MeV (depth)

$^1S_0$: interaction between two nucleons in states of time reversal with $S = L = 0$, and thus in a singlet state.

(QM: ZPF ($\Delta p \Delta x \gtrsim \hbar$) $\frac{\hbar^2}{Ma^2}$)

constituents	M/M_n	a (cm)	v_0 (eV)	Q	phase (T=0)	T_c
^3He	3	2.9 (-8)	8.6 (-4)	0.19	liquid [a)]	
^4He	4	2.9 (-8)	8.6 (-4)	0.14	liquid [a)]	
H_2	2	3.3 (-8)	32 (-4)	0.06	solid [a)]	
^{20}Ne	20	3.1 (-8)	31 (-4)	0.007	solid	
nucleons	1	9 (-14)	100 (+6)	0.5 [c)]	liquid [a,b)]	

a) liquid (condensed)
b) better, Non-Newtonian solid
c) Nucleus, paradigm of quantal many-body Fermi systems.

(B.R. Mottelson, Elementary features of nuclear structure, Les Houches, Session LXVI, Elsevier (1998))

Fluctuations, quantal or classical, favor symmetry: gases and liquids are homogenous. Potential energy on the other hand prefers special arrangements: atoms like to be at specific distances from each other (spontaneous breaking of symmetry).

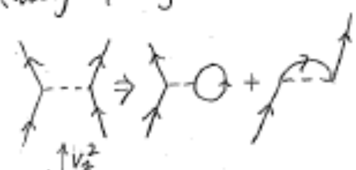

$$U(r) = \int d^3r' \rho(r') v(|r - r'|)$$

$$\rho(r) = \sum_i |\varphi_i(\vec{r})|^2$$

$$U_x = -\sum_i \varphi_i^*(\vec{r}') v(|\vec{r} - \vec{r}'|)\varphi_i(\vec{r})$$

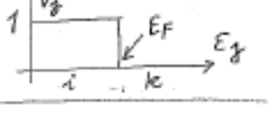

For $Q \gtrsim 0.15$ independent-particle motion.

Figure 0.1.1:

Cooper pairs

~~box 2~~ App. 2.B

HF

$$H = \sum_{j_1 j_2} \langle j_1 | T | j_2 \rangle a^{+}_{j_1} a_{j_2} + \frac{1}{4} \sum_{\substack{j_1 j_2 \\ j_3 j_4}} \langle j_1 j_2 | v | j_3 j_4 \rangle a^{+}_{j_2} a^{+}_{j_1} a_{j_3} a_{j_4}$$

$$j (\equiv j, m)$$

independent particle motion ($Q = 1/2$), mean field

$$a^{+}_{j_2} a^{+}_{j_1} a_{j_3} a_{j_4} \Rightarrow a^{+}_{j_2} \langle a^{+}_{j_1} a_{j_3} \rangle a_{j_4} + \ldots$$

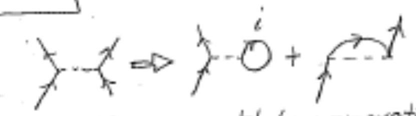

$$\boxed{\begin{aligned} U(r) &= \int d^3r' \rho(r') v(|\vec{r} - \vec{r}'|) \\ U_x(r, r') &= -\sum_i \varphi_i^{*}(\vec{r}') v(|\vec{r} - \vec{r}'|) \varphi_i(\vec{r}) \\ \rho(r) &= \sum_i |\varphi_i(\vec{r})|^2 ; \int d^3r\, \rho(r) = N \end{aligned}}$$

Hartree-Fock, complete separation between occupied ($|i\rangle$) and empty ($|k\rangle$) states

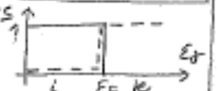

$$(U_\nu^2 + V_\nu^2 = 1) \quad \varphi = \bar{a}^{+}_{\nu} |0\rangle = (U_\nu + V_\nu a^{+}_{\nu}) |0\rangle ; \quad V_\nu^2 = \begin{cases} 1 & \varepsilon_i \le \varepsilon_F \\ 0 & \varepsilon_i > \varepsilon_F \end{cases}$$

$$|\mathrm{Nilsson}(\Omega)\rangle_{\mathcal{K}} = \det(\varphi_\nu) = \prod \bar{a}^{+}_{\nu} |0\rangle = \prod a^{+}_{i} |0\rangle = \prod a^{+}_{i} a^{+}_{\tilde{i}} |0\rangle$$

$$|IKM\rangle \sim \int d\Omega\, \mathcal{D}^{I}_{MK}(\Omega) |\mathrm{Nilsson}(\Omega)\rangle ; \quad E_I = (\hbar^2 / 2\mathcal{J}) I(I+1) ; \quad \mathcal{J} = \mathcal{J}_{rig}$$

independent pair motion

constant m.els approx. $\langle j_1 j_2 | v | j_3 j_4 \rangle = -G$

$$\sum \langle a^{+}_{j_2} a^{+}_{j_1} \rangle a_{j_3} a_{j_4} + \sum a^{+}_{j_2} a^{+}_{j_1} \langle a_{j_3} a_{j_4} \rangle ; \quad \varphi_j^{\mathrm{COOPER}} = (U_j + V_j a^{+}_{jm} a^{+}_{j\tilde{m}}) |0\rangle$$

$$|BCS\rangle = \prod_{jm>0} (U_j + V_j a^{+}_{jm} a^{+}_{j\tilde{m}}) |0\rangle ; \quad \alpha_0 = \langle BCS | \sum_{jm>0} a^{+}_{jm} a^{+}_{j\tilde{m}} | BCS \rangle$$

$$U_\nu = |U_\nu| = U'_\nu ; \quad V_\nu = e^{-2i\phi} V'_\nu \; (V'_\nu \equiv |V_\nu|) \quad (\nu \equiv j, m)$$

$$|BCS(\phi)\rangle_{\mathcal{K}} = \prod_{\nu>0} (U'_\nu + V'_\nu e^{-2i\phi} a^{+}_{\nu} a^{+}_{\tilde{\nu}}) |0\rangle$$

$$= \prod_{\nu>0} (U'_\nu + V'_\nu a'^{+}_{\nu} a'^{+}_{\tilde{\nu}}) |0\rangle = |BCS(\phi = 0)\rangle_{\mathcal{K}'}$$

$\mathcal{K}$: lab. system
$\mathcal{K}'$: intr. system

$$\alpha_0 = \alpha'_0 e^{-2i\phi} ; \quad \alpha'_0 = \sum_{\nu>0} U'_\nu V'_\nu ; \quad \left. \begin{matrix} V'_\nu \\ U'_\nu \end{matrix} \right\} = \frac{1}{\sqrt{2}} \left(1 \mp \frac{1}{E_\nu} \right)^{1/2}$$

$$\Delta = G \alpha_0 ; \quad N_0 = 2 \sum_{\nu>0} V_\nu^2 ; \quad \frac{1}{G} = \sum_{\nu>0} \frac{1}{2E_\nu} \qquad E_\nu = ((\varepsilon_\nu - \lambda)^2 + \Delta^2)^{1/2}$$

$$|N_0\rangle \sim \int_0^{2\pi} d\phi\, |BCS(\phi)\rangle_{\mathcal{K}} \sim \left(\sum_{\nu>0} c_\nu a^{+}_{\nu} a^{+}_{\tilde{\nu}} \right)^{N_0/2} |0\rangle ; \quad E_N = (\hbar^2 / 2\mathcal{J}) N^2$$

$$\mathcal{J} \approx 2\hbar^2 / G$$

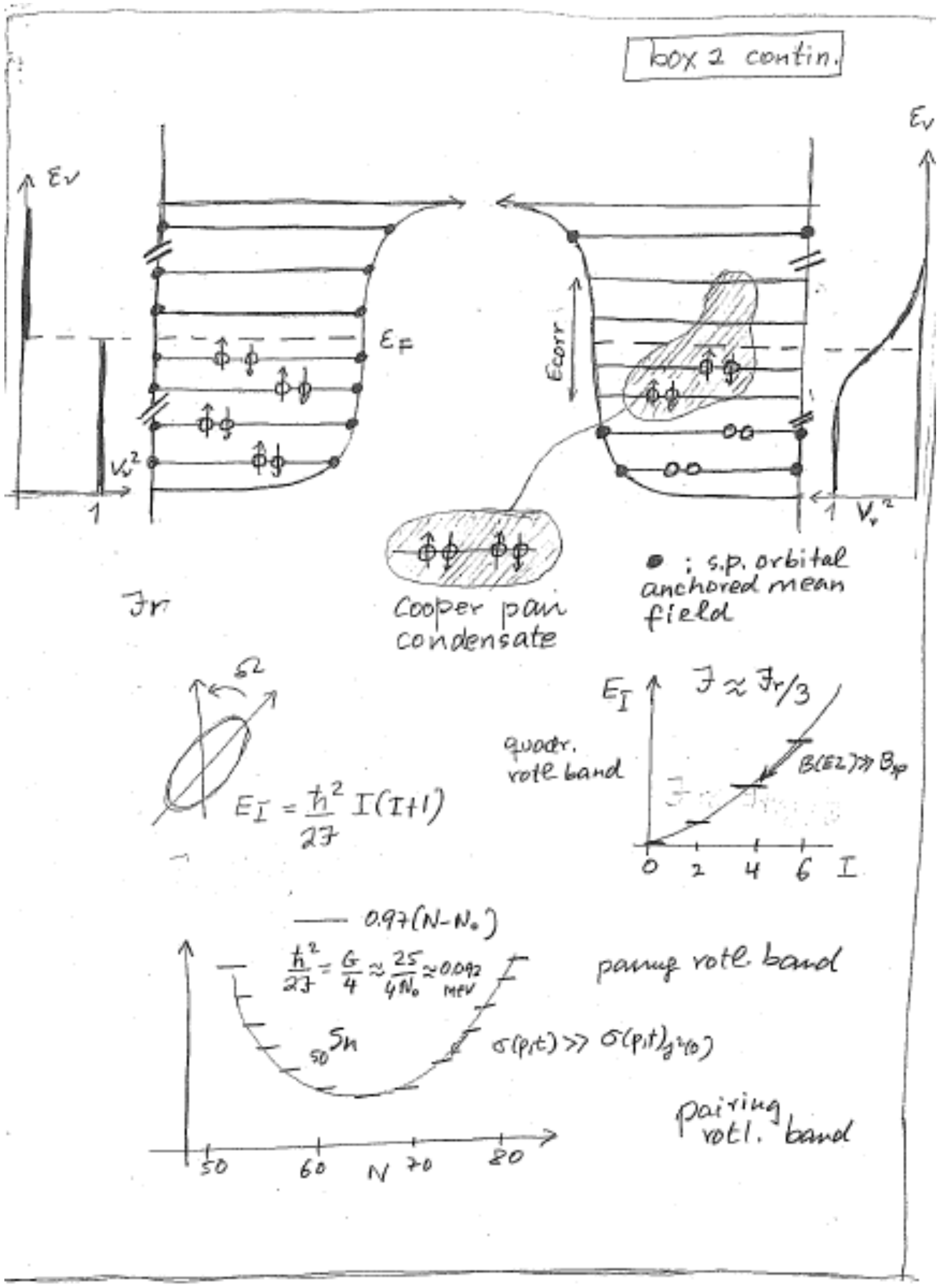
box 2 contin.
E_ν
E_F
E_{corr}
V_ν^2
1
Cooper pair condensate
• ; s.p. orbital anchored mean field
$\mathcal{J}_r$
Ω
$E_I = \frac{\hbar^2}{2\mathcal{J}} I(I+1)$
E_I
$\mathcal{J} \approx \mathcal{J}_r/3$
quadr. rotl. band
$B(E2) \gg B_{sp}$
0 2 4 6 I
— 0.97(N-N₀)
$\frac{\hbar^2}{2\mathcal{J}} = \frac{G}{4} \approx \frac{25}{4N_0} \approx 0.092$ MeV
pairing rotl. band
$_{50}Sn$
$\sigma(p,t) \gg \sigma(p,t)_{sp}$
pairing rotl. band
50 60 N 70 80

Figure 0.1.2:

Two-nucleon spectroscopic amplitudes associated with pairing vibrational modes in closed shell systems $\boxed{\text{box 3}}$ I App. 2C

The solution of the pairing Hamiltonian

$$H = H_{sp} + H_p ,$$

where

$$H_{sp} = \sum_{\nu} \varepsilon_{\nu} a^{\dagger}_{\nu} a_{\nu}$$

and

$$H_p = -G P^{\dagger} P ,$$

with

$$P^{\dagger} = \sum_{\nu > 0} a^{\dagger}_{\nu} a^{\dagger}_{\tilde{\nu}} ,$$

in the Harmonic approximation (RPA) leads to pair addition (a) / a pair removal (r) two-particle, two-hole correlated mode, the associated creation and annihilation operators being

$$\Gamma^{\dagger}_{a}(n) = \sum_{k} X^{a}_{n}(k)\, \Gamma^{\dagger}_{k} + \sum_{i} Y^{a}_{n}(i)\, \Gamma_{i}$$

and

$$\Gamma^{\dagger}_{r}(n) = \sum_{i} X^{r}_{n}(i)\, \Gamma^{\dagger}_{i} + \sum_{k} Y^{r}_{n}(k)\, \Gamma_{k} ,$$

with

$$\sum X^2 - \sum Y^2 = 1$$

and

$$\Gamma^{\dagger}_{k} = a^{\dagger}_{k} a^{\dagger}_{\tilde{k}} , \qquad (\varepsilon_k > \varepsilon_F),$$

$$\Gamma^{\dagger}_{i} = a_{\tilde{i}}\, a_i . \qquad (\varepsilon_k \leq \varepsilon_F).$$

The relations

$$[H, \Gamma^{\dagger}_{a}(n)] = \hbar W_n (\beta = +2)$$

(and

box 3 cont. (II)

$$[H, \Gamma_\nu^\dagger(n)] = \hbar W_n (\beta = -2),$$

where β is the transfer quantum, while n labels the roots of the corresponding dispersion relation

$$\frac{1}{G(\pm 2)} = \sum_k \frac{(\Omega_k/2)}{2\varepsilon_k \mp W_n(\pm 2)} + \sum_i \frac{(\Omega_i/2)}{2\varepsilon_i \pm W_n(\pm 2)}$$

in increasing order of energy.

For the case of the (neutron) pair addition and pair substraction modes of ^{208}Pb the above equation can be graphically solved (cf. Fig. 1), the minimum of the dispersion relation coincides with the Fermi energy. One then obtains

Box 3 3

$$X_1^r(i) = \frac{\frac{1}{2}\Omega_i^{1/2}\Lambda_1(-2)}{2(|\varepsilon_i| - |\varepsilon_{p1/2}|) + E_{corr}(-2)} \; ; \; Y_1^r(k) = \frac{\frac{1}{2}\Omega_k^{1/2}\Lambda_1(-2)}{2(|\varepsilon_{g9/2}| - |\varepsilon_k|) + 2(|\varepsilon_{p1/2}| - |\varepsilon_{g9/2}|) + E_{corr}(-2)}$$

$E_{corr}(-2) = 0.5\,\mathrm{MeV}$ (cf. Fig. 1) $\quad \Omega = j + 1/2$

$2(|\varepsilon_{p1/2}| - |\varepsilon_{g9/2}|) = 6.82\,\mathrm{MeV}$ $\quad 2(|\varepsilon_{p1/2}| - |\varepsilon_{g9/2}|) - E_{corr} = (6.82 - 0.5)\,\mathrm{MeV} = 6.32\,\mathrm{MeV}$

Thus

$$\begin{cases} X_1^r(i) = \dfrac{\frac{1}{2}\Omega_i^{1/2}\Lambda_1(-2)}{2(|\varepsilon_i| - |\varepsilon_{p1/2}|) + 0.5\,\mathrm{MeV}} \; ; \\[2ex] Y_1^r(k) = -\dfrac{\frac{1}{2}\Omega_k^{1/2}\Lambda_1(-2)}{2(|\varepsilon_{g9/2}| - |\varepsilon_k|) + 6.23\,\mathrm{MeV}} \end{cases}$$

Table 2.C.1

units		MeV	MeV^{-1}		TDA
nlj	Ω_i	$\lvert\varepsilon_i\rvert - \lvert\varepsilon_{p1/2}\rvert$	$A(i) = \frac{\frac{1}{2}\Omega_i^{1/2}}{2(\lvert\varepsilon_i\rvert - \lvert\varepsilon_{p1/2}\rvert) + 0.5\,\mathrm{MeV}}$	$X_1^r(i)$	$X_1^r(i)$
$2p_{1/2}$	1	0	1	0.83	0.80
$1f_{5/2}$	3	0.57	0.528	0.44	0.42
$2p_{3/2}$	2	0.90	0.307	0.25	0.25
$0i_{13/2}$	7	1.64	0.350	0.29	0.28
$1f_{7/2}$	4	2.35	0.192	0.16	0.15
$nh_{9/2}$	5	3.87	0.150	0.12	0.12

$\sum A^2(i) = 1.5549$

Very similar to column labeled ^{208}Pb Table [illegible] adv. AP

$\frac{1}{\sqrt{1.5549}} = 0.802 \leftarrow \sum [X_1^r(i)]^{TD} = 1$

units		$\lvert E\rvert$ MeV	MeV^{-1}	
nlj	Ω_k	$\lvert\varepsilon_{g9/2}\rvert - \lvert\varepsilon_k\rvert$	$B(k) = \frac{\frac{1}{2}\Omega_k^{1/2}\Lambda_1(-2)}{2(\lvert\varepsilon_{g9/2}\rvert - \lvert\varepsilon_k\rvert) + 6.23\,\mathrm{MeV}}$	$Y_1^r(i)$
$1g_{9/2}$	5	0	0.179	−0.15
$0i_{11/2}$	6	0.77	0.158	−0.13
$0j_{15/2}$	8	1.41	0.156	−0.13
$2d_{5/2}$	3	1.56	0.093	−0.08
$3s_{1/2}$	1	2.03	0.046	−0.04
$1g_{7/2}$	4	2.47	0.090	−0.07
$2d_{3/2}$	2	2.51	0.063	−0.05

$\sum B^2(k) = 0.10418$

$\Lambda_1(-2) = 0.83025$ MeV $\quad \Lambda_1^2(-2)\left(\sum_i A^2(i) - \sum_k B^2(k)\right) = \Lambda_1^2(-2)(1.5549 - 0.10418)$

$= \Lambda_1^2(-2)\, 1.45073 = 1$

$W_1(+2) = 2(\varepsilon_{g9/2} - \varepsilon_F) - E_{corr}(+2)$

all energies which enter X, Y are positive

(4)

Box 3

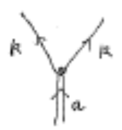

$$X_1^a(k) = \frac{\frac{1}{2}\Omega_k^{1/2}\Lambda_1(+2)}{2(\varepsilon_k - \varepsilon_F) - W_1(+2)}$$

$$2(\varepsilon_k - \varepsilon_F) - W_1(+2) = \cancel{[illegible]}$$

$$= 2(\varepsilon_k - \cancel{\varepsilon_F}) - \left(2(\varepsilon_{g9/2} - \cancel{\varepsilon_F}) - E_{corr}(+2)\right)$$

$$= 2(\varepsilon_k - \varepsilon_{g9/2}) + E_{corr}(+2)$$

$$= 2(|\varepsilon_{g9/2}| - |\varepsilon_k|) + E_{corr}(+2)$$

$$\boxed{X_1^a(k) = \frac{\frac{1}{2}\Omega_k^{1/2}\Lambda_1(+2)}{2(|\varepsilon_{g9/2}| - |\varepsilon_k|) + E_{corr}(+2)}}$$

$$Y_1^a(i) = -\frac{\frac{1}{2}\Omega_i^{1/2}\Lambda_1(+2)}{2(\varepsilon_F - \varepsilon_i) + W_1(+2)}$$

$$2(\varepsilon_F - \varepsilon_i) + W_1(+2) = 2(\cancel{\varepsilon_F} - \varepsilon_i) + 2(\varepsilon_{g9/2} - \cancel{\varepsilon_F}) - E_{corr}(+2)$$

$$= 2(\varepsilon_{p1/2} - \varepsilon_i) + 2(\varepsilon_{g9/2} - \varepsilon_{p1/2}) - E_{corr}(+2)$$

$$= 2(|\varepsilon_i| - |\varepsilon_{p1/2}|) + \underbrace{2\,\underbrace{(|\varepsilon_{p1/2}| - |\varepsilon_{g9/2}|)}_{\text{s.p. gap } 3.41\,\text{MeV}}}_{6.28\,\text{MeV}} - \underbrace{E_{corr}(+2)}_{1.248\,\text{MeV (see Fig. 1)}}$$

~~const~~ ~~$E_{corr}(+2) = 1.5$ MeV~~

OK $$\boxed{\cancel{Y_1^a(i) = -}\frac{\frac{1}{2}\Omega_i^{1/2}\Lambda_1(+2)}{2(|\varepsilon_i| - |\varepsilon_{p1/2}|) + 5.032\,\text{MeV}}}$$

$$\boxed{Y_1^a(i) = -\frac{\frac{1}{2}\Omega_i^{1/2}\Lambda_1(+2)}{2(|\varepsilon_i| - |\varepsilon_{p1/2}|) + 2\Delta\varepsilon_{sp} - E_{corr}(+2)}}$$

$\Delta\varepsilon_{sp}$ = single-particle closed shell gap > 0

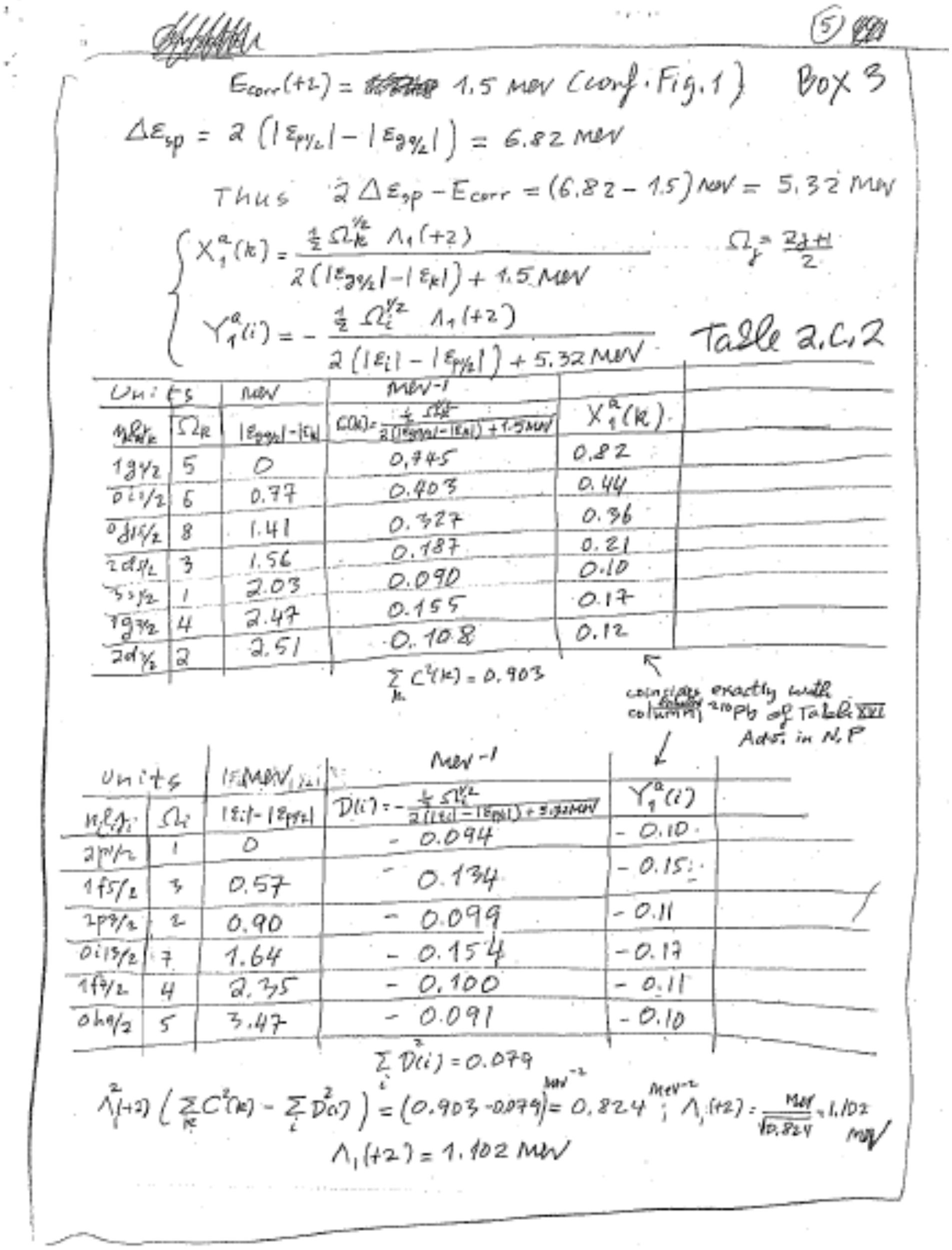

(5)

$E_{corr}(+2) = 1.5$ MeV (conf. Fig. 1) Box 3

$\Delta\varepsilon_{sp} = 2\left(|\varepsilon_{p_{1/2}}| - |\varepsilon_{g_{9/2}}|\right) = 6.82$ MeV

Thus $2\Delta\varepsilon_{sp} - E_{corr} = (6.82 - 1.5)$ MeV $= 5.32$ MeV

$$\begin{cases} X_1^a(k) = \dfrac{\frac{1}{2}\Omega_k^{1/2}\,\Lambda_1(+2)}{2\left(|\varepsilon_{g_{9/2}}| - |\varepsilon_k|\right) + 1.5\text{ MeV}} \\ Y_1^a(i) = -\dfrac{\frac{1}{2}\Omega_i^{1/2}\,\Lambda_1(+2)}{2\left(|\varepsilon_i| - |\varepsilon_{p_{1/2}}|\right) + 5.32\text{ MeV}} \end{cases} \qquad \Omega_j = \frac{2j+1}{2}$$

Table 2.C.2

Units		MeV	MeV^{-1}	
$n l_k j_k$	Ω_k	$\lvert\varepsilon_{g_{9/2}}\rvert - \lvert\varepsilon_k\rvert$	$C(k) = \frac{\frac{1}{2}\Omega_k^{1/2}}{2(\lvert\varepsilon_{g_{9/2}}\rvert - \lvert\varepsilon_k\rvert) + 1.5\text{ MeV}}$	$X_1^a(k)$
$1g_{9/2}$	5	0	0.745	0.82
$0i_{11/2}$	6	0.77	0.403	0.44
$0j_{15/2}$	8	1.41	0.327	0.36
$2d_{5/2}$	3	1.56	0.187	0.21
$3s_{1/2}$	1	2.03	0.090	0.10
$1g_{7/2}$	4	2.47	0.155	0.17
$2d_{3/2}$	2	2.51	0.108	0.12

$\sum_k C^2(k) = 0.903$

coincides exactly with column ^{210}Pb of Table XXI Adv. in N.P

Units		MeV	MeV^{-1}	
$n l_i j_i$	Ω_i	$\lvert\varepsilon_i\rvert - \lvert\varepsilon_{p_{1/2}}\rvert$	$D(i) = -\frac{\frac{1}{2}\Omega_i^{1/2}}{2(\lvert\varepsilon_i\rvert - \lvert\varepsilon_{p_{1/2}}\rvert) + 5.32\text{ MeV}}$	$Y_1^a(i)$
$2p_{1/2}$	1	0	−0.094	−0.10
$1f_{5/2}$	3	0.57	−0.134	−0.15
$2p_{3/2}$	2	0.90	−0.099	−0.11
$0i_{13/2}$	7	1.64	−0.154	−0.17
$1f_{7/2}$	4	2.35	−0.100	−0.11
$0h_{9/2}$	5	3.47	−0.091	−0.10

$\sum_i D^2(i) = 0.079$

$\Lambda_1^2(+2)\left(\sum_k C^2(k) - \sum_i D^2(i)\right) = (0.903 - 0.079) = 0.824$ MeV^{-2}; $\Lambda_1(+2) = \frac{\text{MeV}}{\sqrt{0.824}} = 1.102$ MeV

$\Lambda_1(+2) = 1.102$ MeV

Figure 0.1.3:

Microscopic mechanism to break gauge invariance

~~Box 4~~ ①

App. 2.D

Pairing is intimately connected with particle number violation and thus spontaneous breaking of gauge invariance, as testified by the order parameter $\langle BCS|P^{\dagger}|BCS\rangle = \alpha_0$. Now, in the nuclear case and at variance with condensed matter, dynamical breaking of gauge symmetry is equally important (pairing vibrations around closed shell nuclei, cf. Fig. 2 box 3). The fact that the average single-particle field acts as an external potential (like e.g. magnetic field in metallic superconductors) is at the basis of of the existence of a critical value of the pairing strength G to bind Cooper pairs in nuclei. In fact, spatial quantization in finite systems at large and in nuclei in particular, intimately connecte with the paramount role the surface has in these systems, is at the basis of the existence of a critical G value. Also of the fact that in nuclei an important fraction (30-50%) of Cooper pair binding an due to the exchange of collective vibrations between the partners of the pair, the rest being associated with the bare NN interaction in the $^1S_0$ channel (cf. Fig. 1)

Now, there are situations in which spatial quantization screens, essentially completely, the NN-interaction. This happens in the case in which the nuclear valence orbitals are s,p-states at threshold (pairing anti-halo effect). Examples of situations of this mechanism

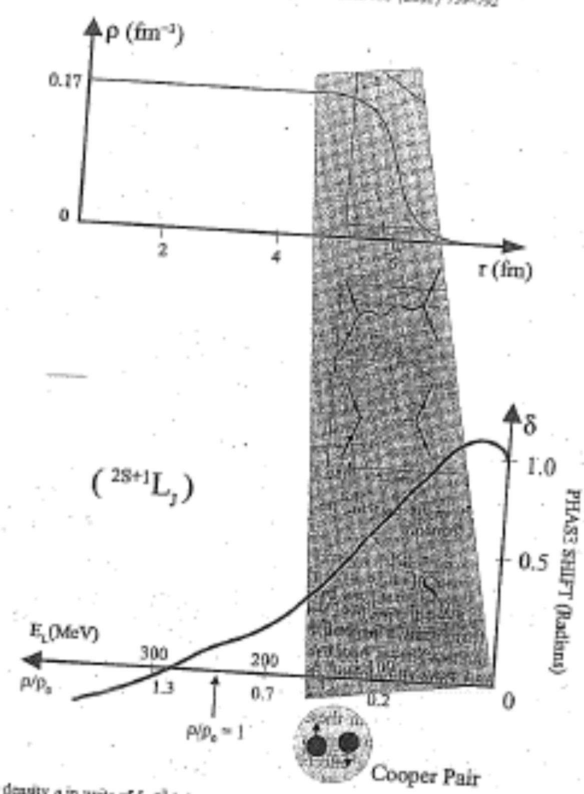

Fig. 13. (top) Nuclear density ρ in units of fm^{-3} (where fm $\equiv 10^{-13}$ cm), plotted as a function of the distance r (in units of fm) from the centre of the nucleus. Saturation density correspond to ≈ 0.17 fm^{-3}, equivalent to 2.8×10^{14} g/cm^3. Because of the short range of the nuclear force, the strong force, the nuclear density changes from 90% of saturation density to 10% within 0.65 fm, i.e. within the nuclear diffusivity. (bottom) Phase parameter associated with the elastic scattering of two nucleons moving in states of time reversal, so called $^1S_0$ phase shift, in keeping with the fact that the system is in a singlet state of spin zero. The solution of the Schrödinger equation describing the elastic scattering of a nucleon from a scattering centre (in this case another nucleon) is, at large distances from the scattering centre a superposition of the incoming wave and of the outgoing, scattering wave. The interaction of the incoming particle with the target particle changes only the amplitude of the outgoing wave. This amplitude can be written in terms of a real phase shift—or scattering phase—δ. Positive values of δ implies an attractive interaction, negative a repulsive one. For low relative velocities (kinetic energies E_L), i.e. around the nuclear surface where the density is low, the $^1S_0$ phase shift arising from the exchange of mesons (like for example pions, represented by an horizontal dotted red line) between nucleons (represented by upward pointing arrowed lines) is attractive. This mechanism provides about half of the glue to nucleons moving in time reversal states to form Cooper pairs. These pairs behaves like boson and eventually condense in a single quantal state leading to nuclear superfluidity. Cooper pair formation is further assisted by the exchange of collective surface vibrations (green wavy curve in the scattering process) between the members of the pair.

type are provided by $N=6$ (parity in- $\boxed{\text{box4}}$ version) isotones. In particular, by ^{11}Li ③, in which case the strongly renormalized $s1/2$ and $p1/2$ valence orbitals are a virtual and a resonant state lying at ≈ 0.1 and 0.6 MeV in the continuum, respectively. In keeping with the fact that the binding provided to a pair of fermions moving in time reversal states by a contact pairing interaction (δ-force) is (cf. e.g. Eq. (2.12) Brink and Broglia (2005)) $E_0 = -(2j+1)/2\, V_0\, I(j) \approx -\frac{(2j+1)}{2} V_0 \frac{3}{R^3}$, the ratio

$$r = \frac{2}{(2j+1)}\left(\frac{R_0}{R}\right)^3,$$

where $R_0 = 1.2 A^{1/3}$ fm $= 2.7$ fm ($A=11$), and $R = \sqrt{\frac{5}{3}}\langle r^2\rangle^{1/2}_{^{11}Li} = \sqrt{\frac{5}{3}}\; 3.74$ fm $= 4.6$ fm are the radius of a stable nucleus of mass $A=11$ (systematics), while R is the measured one, while j is the angular momentum representative for a nucleus of mass $A=11$ ($j \sim k_F R_0 \approx 3$-4), one obtains $r = 0.06$.

Making use of the multipole expansion of a general interaction

$$v(|\vec{r}_1 - \vec{r}_2|) = \sum_\lambda V_\lambda(r_1, r_2) P_\lambda(\cos\theta_{12}),$$

Because the function P_λ drops from its maximum at $\theta_{12}=0$ in an angular distance $1/\lambda$, particles 1 and 2 interact through the component λ of the force, only if $r_{12} = |\vec{r}_1 - \vec{r}_2| < R/\lambda$, where R is the mean value of the radii $\vec{r}_1$ and $\vec{r}_2$. Thus, as λ increases, the effective force range decreases. For a force of range much greater than the nuclear size, only the $\lambda = 0$ term is important. At the other extreme, a δ-function force has coefficients $V_\lambda(r_1, r_2)$ $\left(= \frac{(2\lambda+1)}{4\pi r_1^2}\delta(r_1 - r_2)\right)$ that increase with λ.

$\boxed{\text{Box 4}}$ (3)

In the case of ^{11}Li(gs) we are thus forced to accept the need for a long range, low λ pairing interaction, as responsible for the binding of the dineutron, halo Cooper pair to the ^{9}Li core. This is equivalent to saying, an induced pairing interaction arising from the exchange of vibrations with low λ-value.

Boostrap Cooper pair binding

Within the s,p subspace, the most natural long wavelength vibration is the dipole mode. From systematics, the centroid of these vibrations is $\hbar\omega_{GDR} \approx 100\,\mathrm{MeV}/R$, R being the nuclear radius. Thus, in the case of ^{11}Li, one expects the centroid of the Giant Dipole Resonance carrying $\approx 100\%$ of the energy weighted sum rule (EWSR) at $\hbar\omega_{GDR} \approx 100\,\mathrm{MeV}/2.7 \approx 37$ MeV. Now, such a high frequency mode can hardly be expected to give rise to anything, but polarization effects. On the other hand, there exists experimental evidence which testifies to the presence of a rather sharp dipole state with centroid at ≈ 1 MeV and carrying $\approx 10\%$ of the

EWSR. The existence of this $\boxed{\text{box 4}}$ (4)
"pigmy resonance" which can be viewed as a simple consequence of the existence of a low-lying particle-hole state associated with the transition $s_{1/2} \to p_{1/2}$, arguably, testifies to the coexistence of two states with rather different radii in the ground state*). One, closely connected with the compact $(\approx 2.7\,fm)$ ^9Li core, the second with the diffuse halo $(\approx 4.6\,fm)$. Because the overlap between them is smal $(\approx (2.7/4.6)^3 \approx 0.2)$, one can posit that a bona fide dipole pigmy resonance is a GDR based on an exotic, unusually extended state as compared to systematics $(A \approx (4.6/1.2)^3 \approx 60)$, i.e. to a system with an effective A mass number about 5 time than predicted by systematics.**)

Let us try to shed some light on these issues. Making use of of the relation $\langle r^2 \rangle^{1/2} \approx (3/5)^{1/2} R$ between mean square radius and radius, one may write

$$\langle r^2 \rangle_{^{11}Li} \approx \frac{3}{5} R_{eff}^2 (^{11}Li),$$

Furthermore, the pigmy dipole resonance may be built not only on the ~~large~~ extended component of the ground state as in ^{11}Li but also on excited ~~state~~ like e.g. ^{12}Be (see Fig. 2.)

*) This is reminiscent of the deformation coexistence found in e.g. ^{16}O, ^{40}Ca ground states and, recently in - - - -

**) Within this context the dipole strength found at ≈ 10 MeV in neutron skin rich nuclei can hardly be consider pigmy resonance, but the long tail of the GDR.

box 4 ⑤

with

$$R_{eff}(^{11}Li) = \left(\frac{9}{11} R_0^2(^9Li) + \frac{2}{11}\left(\frac{\xi}{2}\right)^2\right),$$

where

$$R_0(^9Li) = 2.5\,\text{fm}$$

is the ^9Li radius ($R_0 = r_0 A^{1/3}$, $r_0 = 1.2$ fm), where ξ is the correlation length of the Cooper pair neutron halo. An estimate of this quantity is provided by the relation

$$\xi = \frac{\hbar v_F}{2E_{corr}} \approx 20\,\text{fm},$$

in keeping with the fact that in ^{11}Li, $(v_F/c) \approx 0.1$ and $E_{corr} \approx 0.5$ MeV. Consequently, $\langle r^2\rangle^{1/2}_{^{11}Li} \approx 3.74$ fm ($R_{eff}(^{11}Li) \approx 4.83$ fm), in overall agreement with the experimental value $\langle r^2\rangle^{1/2}_{^{11}Li} = 3.55 \pm 0.1$ fm (Kobayashi et al., 1989).

We now procede to the calculation of the centroid of the dipole pigmy resonance of ^{11}Li. Making use of the dispersion relation given in Eq. (3.30) p.55 of Bortignon et al, 1998, and of the fact that $\varepsilon_{1/2} - \varepsilon_{1/2} = \varepsilon_{p1/2} - \varepsilon_{s1/2} \approx 0.5$ MeV (see Fig. 11.1 p. 264 Brink and Broglia (2010)),

Brink D.M and R.A. Broglia (2010) Nuclear Superfluidity, Cambridge University Press, Cambridge,
Kobayashi .... (1989) Phys. Lett. B 332, 51)
Bortignon, P.F., A. Bracco and R.A. Broglia (1998) Giant Resonances, Harwood Academic Publishers, Amsterdam,

box 4 (6)

and that the EWSR associated with the ^{11}Li pigmy resonance is $\approx 10\%$ of the total Thomas-Reiche-Kuhn sum rule one can write,

$$0.1\,\frac{\hbar^2 A}{2M} = \frac{1}{K_1}\left[(0.5\,\mathrm{MeV})^2 - (\hbar\omega_{pigmy})^2\right],$$

and thus

$$(\hbar\omega_{pigmy})^2 = (0.5\,\mathrm{MeV})^2 - 0.1\,\frac{\hbar^2 A}{2M}\,K_1,$$

where (see Bortignon et al (1998))

$$K_1 = -\frac{5V_1}{A(3/2)^2}\left(\frac{2}{11}\right) = -\frac{125\,\mathrm{MeV}}{A\times 100\,\mathrm{fm}^2}\left(\frac{2}{11}\right) \approx -\frac{2.5}{A^2}\,\mathrm{fm}^{-2}\,\mathrm{MeV},$$

the ratio in parenthesis reflecting the fact that only 2 out of 11 nucleons, slosh back and forth in an extended configuration with little overlap with the other nucleons. One then obtains,

$$-0.1\,\frac{\hbar^2 A}{2M}\,K_1 = 0.1\times 20\,\mathrm{MeV\,fm}^2\,A\times\frac{2.5}{A^2}\,\mathrm{fm}^{-2}\,\mathrm{MeV}$$
$$\approx 0.45\,\mathrm{MeV} \approx (0.7\,\mathrm{MeV})^2$$

consequently

$$\hbar\omega_{pigmy} = \sqrt{(0.5)^2+(0.7)^2}\,\mathrm{MeV} \approx 1\,\mathrm{MeV},$$

box 4 ⑦

in overall agreement with the experimental findings (Zinser et al, 1997). It is of notice that the centroid of the pigmy resonance calculated in the RPA with the help of a separable interaction is $\approx (0.8\,\mathrm{MeV} + 2.0\,\mathrm{MeV})/2 \approx 1.4\,\mathrm{MeV}$ (see Fig. 11.3(a) p. 269, Brink and Broglia, 2010).

Let us now estimate the binding which the exchange of the pigmy resonance between two neutron of the Cooper pair halo of ^{11}Li can provide

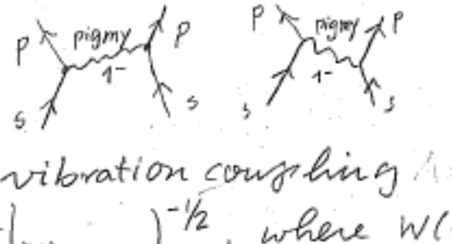

The associated particle vibration coupling $\Lambda = \left(\partial W(E)/\partial E\big|_{\hbar\omega_{pigmy}}\right)^{-1/2}$, where $W(E)$ is the dispersion relation used to determine $\hbar\omega_{pigmy}$ (cf. e.g. Brink and Broglia Eq. (8.42) p. 189; (note the use of a dimensionless dipole single particle field $F'_{dim} = F/\langle r^2\rangle_{^{11}Li}$]

$$W(E) = \sum_{\nu_k \nu_i} \frac{2(\varepsilon_k - \varepsilon_i)\,|\langle \tilde{i}|F/\langle r^2\rangle_{^{11}Li}|k\rangle|^2}{(\varepsilon_k - \varepsilon_i)^2 - E^2}$$

Zinser et al 1997 Nucl. Phys. A619, 151.

box 4 (8)

One then obtains

$$\Lambda^2 = \left\{ 2\hbar\omega_{pigmy} \frac{0.1(TRK)/\langle r^2\rangle_{^{11}Li}}{[(\varepsilon_{p1/2}-\varepsilon_{s1/2})^2-(\hbar\omega_{pigmy})^2]^2} \right\}^{-1}$$

$$= \left\{ 2\,MeV \frac{0.1(\hbar^2/2M)(1/\langle r^2\rangle_{^{11}Li})}{[(0.5)^2-(1MeV)^2]^2 MeV^4} \right\}^{-1}$$

$$= \left(\frac{0.75}{1.57}\right)^2 = 0.48\ MeV^2$$

leading to $\Lambda = 0.7$ MeV. The value of induced interaction matrix element is then given by

$$M_{ind} = -\frac{\Lambda^2}{\hbar\omega_{pigmy}} = -0.5\ MeV,$$

and the same contribution for the other time ordering. Assuming the halo neutrons to spend the same amount of time in the $|s_{1/2}^2(0)\rangle$ ($\varepsilon_{s1/2}=0.1MeV$) than in the $|p_{1/2}^2(0)\rangle$ ($\varepsilon_{p1/2}=0.6$ MeV) configuration, the correlation energy is $E_{corr} = |2(\varepsilon_{s1/2}+\varepsilon_{p1/2})/2+2M_{ind}| = 0.3$ MeV, in overall agreement with the findings (0.380 MeV, reference).

2,24 MeV

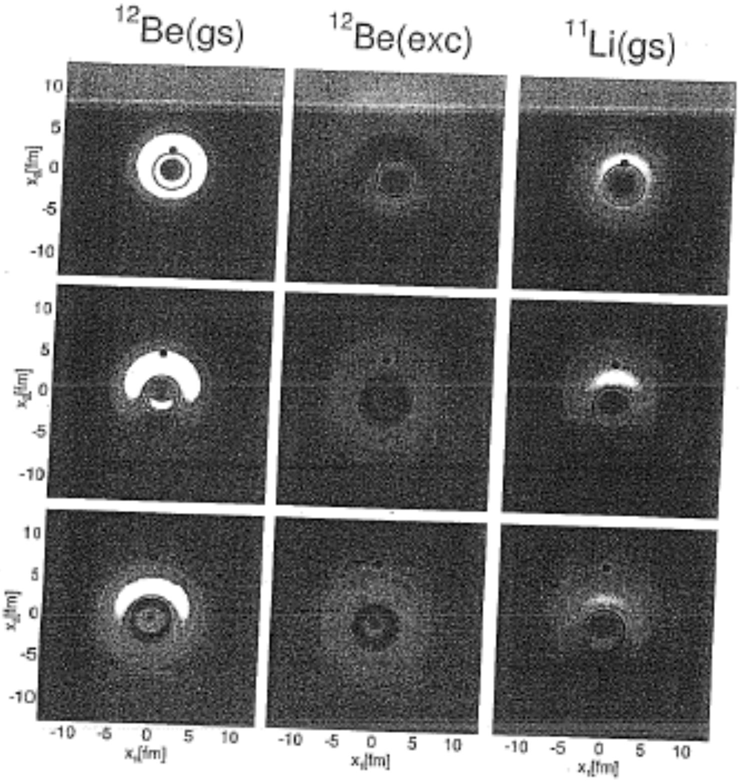

$$|0\rangle_\nu = |0\rangle + \alpha|(p,s)_{1^-} \otimes 1^-;0\rangle + \beta|(s,d)_{2^+} \otimes 2^+;0\rangle + \gamma|(p,d)_{3^-} \otimes 3^-;0\rangle$$

$$|0\rangle_\nu = a|s^2(0)\rangle + b|p^2(0)\rangle + c|d^2(0)\rangle$$

	^{11}Li(gs)	^{12}Be(gs)	^{12}Be(exc)
α	0.7	0.10	0.08
β	0.1	0.30	-0.39
γ	–	0.37	-0.1
a	0.45	0.37	0.89
b	0.55	0.50	0.17
c	0.04	0.60	0.19

$\boxed{\text{exotic decay}}$ →

← pigmy resonance in Pb

$s^2(0)$

at threshold

Figure 0.1.4:

Bibliography

R. Broglia, O. Hansen, and C. Riedel. Two–neutron transfer reactions and the pairing model. *Advances in Nuclear Physics*, 6:287, 1973. URL `http://merlino.mi.infn.it/repository/BrogliaHansenRiedel.pdf`.

G. Potel, A. Idini, F. Barranco, E. Vigezzi, and R. A. Broglia. Cooper pair transfer in nuclei. *Rep. Prog. Phys.*, 76:106301, 2013.